

Robust Image Registration using Mixtures of t -distributions

Demetrios Gerogiannis *

Christophoros Nikou

Aristidis Likas

University of Ioannina,
Department of Computer Science,
PO Box 1185, 45110 Ioannina, Greece,
{dgerogia,cnikou,arly}@cs.uoi.gr

Abstract

We propose a pixel similarity-based algorithm enabling accurate rigid registration between single and multimodal images presenting gross dissimilarities due to noise, missing data or outlying measures. The method relies on the partitioning of a reference image by a Student's t -mixture model (SMM). This partition is then projected onto the image to be registered. The main idea is that a t -component in the reference image corresponds to a t -component in the image to be registered. If the images are correctly registered the weighted sum of distances between the corresponding components is minimized. The use of SMM components is justified by the property that they have heavier tails than standard Gaussians, thus providing robustness to outliers. Experimental results indicate that, even in the case of images presenting low SNR or important amount of dissimilarities due to temporal changes, the proposed algorithm compares favorably to the histogram-based mutual information method that is widely used in a variety of applications.

1. Introduction

The goal of image registration is to geometrically align two or more images in order to superimpose pixels representing the same underlying structure. Image registration is an important preliminary step in many application fields involving, for instance, the detection of changes in temporal image sequences or the fusion of multimodal images. For the state of the art of registration methods we refer the reader to [29]. Medical imaging, with its wide variety of sensors (MRI, nuclear, ultrasonic, X-Ray) is probably one of the first application fields [18, 1, 9]. Other research areas related to image registration are remote sensing, multisensor robot vision and multisource imaging used in the preser-

vation of artistic patrimony. Respective applications include the following of the evolution of pathologies in medical image sequences [22], the detection of changes in urban development from aerial photographs [14] and the recovery of underpaintings from visible/X-ray pairs of images in fine arts painting analysis [10].

The overwhelming majority of change detection or data fusion algorithms assume that the images to be compared are perfectly registered. Even slightly erroneous registrations may become an important source of interpretation errors when inter-image changes have to be detected. Accurate (i.e. subpixel or subvoxel) registration of single modal images remains an intricate problem when gross dissimilarities are observed. The problem is even more difficult for multimodal images, showing both localized changes that have to be detected and an overall difference due to the variety of responses by multiple sensors.

Since the seminal works of Viola and Wells [28] and Maes *et al.* [17], the maximization of the mutual information measure between a pair of images has gained an increasing popularity as a criterion for image registration [24]. The estimation of both marginal and joint probability density functions of the involved images is a key element in mutual information based image alignment. However, this method is limited by the histogram binning problem. Approaches to overcome this limitation include Parzen windowing [28, 13], where we have the problem of kernel width specification, and spline approximation [27, 19]. A recently proposed method relies on the continuous representation of the image function and develops a relation between image intensities and image gradients along the level sets of the respective intensity [25].

Gaussian mixture modeling (GMM) [4, 20] constitutes a powerful and flexible method for probabilistic data clustering that is based on the assumption that the data of each cluster has been generated by the same Gaussian component. In [16], GMMs were trained off-line to provide prior information on the expected joint histogram when the im-

*This work was partially supported by Interreg IIIA (Greece-Italy) grant I2101005.

ages are correctly registered. GMMs have also been successfully used as models for the joint [8] as well as the marginal image densities [11], in order to perform intensity correction. They have also been applied in the registration of point sets [15] without establishing explicit correspondence between points in the two images. The parameters of GMMs can be estimated very efficiently through maximum likelihood (ML) estimation using the EM algorithm [8]. Furthermore, it is well-known that GMMs are capable of modeling any pdf [20].

An important issue in image registration is the existence of outlying data due to temporal changes (e.g. urban development in satellite images, lesion evolution in medical images) or even the complimentary but non redundant information in pairs of multimodal images (e.g. visible and infrared data, functional and anatomical medical images). Although a large variety of image registration methods have been proposed in the literature only a few techniques address these cases [12, 22, 26].

The method proposed in this study is based on mixture model training. More specifically, we train a mixture model once for the reference image and obtain the corresponding partitioning of image pixels into clusters. Each cluster is represented by the parameters of the corresponding density component. The main idea is that a component in the reference image corresponds to a component in the image to be registered. If the images are correctly registered the sum of distances between the corresponding components is minimum.

A straightforward implementation of the above idea would consider models with Gaussian components. However, it is well known that GMMs are sensitive to outliers and may lead to excessive sensitivity to small numbers of data points. This is easily understood by recalling that maximization of the likelihood function under an assumed Gaussian distribution is equivalent to finding the least-squares solution which lacks robustness. Consequently, a GMM tends to over-estimate the number of clusters since it uses additional components to capture the tails of the distributions [3]. The problem of attaining robustness against outliers in multivariate data is difficult and increases with the dimensionality. In this paper, we consider mixture models (SMM) with Student's- t components for image registration. This pdf has heavier tails compared to a Gaussian [23]. More specifically, each component in the SMM mixture originates from a wider class of elliptically symmetric distributions with an additional parameter called the number of degrees of freedom. In this way, a more robust mixture model is employed than the typical GMM.

The main contributions of the proposed registration method are the following: (i) the histogram binning problem is overcome through image modeling with mixtures of distributions which provide a continuous representation

of image density. (ii) Robustness to outlying pixel values is achieved by using mixtures of Student's t -distributions. The widely used method of maximization of the mutual information is outperformed. (iii) The method may be directly applied to vector valued images (e.g. diffusion tensor MRI) where standard histogram-based method fail due to *the curse of dimensionality*. (iv) The proposed method is faster than histogram based methods where the joint histogram needs to be computed at every change in the transformation parameters.

The remainder of this paper is organized as follows. In section 2, we present our image registration method for general mixture models. ML estimation of the parameters of a Student's t -mixture model and implementation issues of the proposed registration algorithm using SMMs are described in section 3. Experimental results and comparison with the state of the art registration method of maximization of the mutual information (MI) are provided in section 4, while conclusions are drawn in section 5.

2. Image registration by minimization of the distance between mixture models

Let I_{ref} be an image of $N \times N$ pixels with intensities denoted as $I_{ref}(x^i)$, where $x^i, i = 1, \dots, N^2$, is the i^{th} pixel. The purpose of rigid image registration is to estimate a set of parameters \mathcal{S} of the rigid transformation $T_{\mathcal{S}}$ minimizing a cost function $E(I_{ref}(\cdot), I_{reg}(T_{\mathcal{S}}(\cdot)))$ that, in a similarity metric-based context, expresses the similarity between the image pair. In the 2D case the rigid transformation parameters are the rotation angle and the translation parameters along the two axes. In the 3D case, there are three rotation and three translation parameters. Eventually, scale factors may also be included, depending on the definition of the transformation.

Consider, now, a partitioning of the reference image I_{ref} into K clusters (groups) by training a mixture model with K components with arbitrary pdf $g(I(x); \Theta)$:

$$\phi(I_{ref}(x)) = \sum_{k=1}^K \pi_k P(I_{ref}(x); \Theta_k^{ref})$$

Therefore, the reference image is represented by the parameters $\Theta_k^{ref}, k = 1, \dots, K$ of the mixture components. The partitioning of the image is described using the function $f(x) : [1, 2, \dots, N] \times [1, 2, \dots, N] \rightarrow \{1, 2, \dots, K\}$, where $f(x) = k$ means that pixel x of the reference image I_{ref} belongs to the cluster defined by the k^{th} component. Let us also define the sets of all pixels of image I_{ref} belonging to the k^{th} cluster:

$$P_k = \{x^i \in I_{ref}, i = 1, 2, \dots, N^2 / \delta(f(x^i) - k) = 1, \}$$

for $k = 1, \dots, K$, where $\delta(x)$ is the Dirac function:

$$\delta(f(x^i) - k) = \begin{cases} 1, & \text{if } f(x^i) = k \\ 0, & \text{otherwise} \end{cases} \quad (1)$$

The above mixture-based segmentation of the reference image is performed once, at the beginning of the registration procedure. The reference image I_{ref} is, thus, partitioned into K groups, generally, not corresponding to connected components in the image. This spatial partition is projected on the image to be registered I_{reg} , yielding the same partition of this second image (i.e., the partitioning of the reference image acts as a mask on the image to be registered). Then, we assume that the pixel values of each cluster k in I_{reg} are modeled using a mixture component with parameters Θ_k^{reg} obtained from the statistics of the intensities of pixels in group k .

In order to apply our method it should be possible to define a distance measure $D(\Theta_k^{ref}, \Theta_k^{reg})$ between the corresponding mixture components with pdf $p(I)$. Then the energy function we propose, is expressed by the weighted sum of distances between the corresponding components in I_{reg} and I_{ref} :

$$E(I_{ref}(\cdot), I_{reg}(T_S(\cdot))) = \sum_{k=1}^K \pi_k D(\Theta_k^{ref}, \Theta_k^{reg}) \quad (2)$$

where π_k is the mixing proportion of the k^{th} component:

$$\pi_k = \frac{|P_k|}{\sum_{l=1}^K |P_l|}$$

where $|P_k|$ denotes the cardinality of set P_k . If the two images are correctly registered the criterion in (2) assumes that the total distance between the whole set of components would be minimum.

For a given set of transformation parameters \mathcal{S} , the total energy between the image pair is computed through the following steps:

- segment the reference image $I_{ref}(\cdot)$ into K clusters by a mixture model.
- for each cluster $k = 1, 2, \dots, K$ of the reference image:
 - project the pixels of the cluster onto the transformed image to be registered $I_{reg}(T_S(\cdot))$.
 - determine the parameters Θ_k^{reg} of the projected partition of I_{reg} .
- evaluate the energy in eq. (2) by computing the distances between the corresponding densities.

For example it is straightforward to apply the above registration procedure in the case of GMMs. Consider the multivariate normal distributions $N_1(\mu_1, \Sigma_1)$ and $N_2(\mu_2, \Sigma_2)$ and denote $\Theta_i = \{\mu_i, \Sigma_i\}$, with $i = \{1, 2\}$, their respective parameters (mean vector and covariance matrix). The Chernoff distance between these distributions is defined as [7]:

$$C(\Theta_1, \Theta_2, s) = \frac{s(1-s)}{2} \Delta\mu^T [s\Sigma_1 + (1-s)\Sigma_2]^{-1} \Delta\mu + \frac{1}{2} \ln \left(\frac{|s\Sigma_1 + (1-s)\Sigma_2|}{|\Sigma_1|^s |\Sigma_2|^{1-s}} \right),$$

where $\Delta\mu = \mu_2 - \mu_1$. The Bhattacharyya distance is a special case of the Chernoff distance with $s = 0.5$:

$$B(\Theta_1, \Theta_2) = \frac{1}{8} \Delta\mu^T \left[\frac{\Sigma_1 + \Sigma_2}{2} \right]^{-1} \Delta\mu + \frac{1}{2} \ln \left(\frac{|\frac{\Sigma_1 + \Sigma_2}{2}|}{\sqrt{|\Sigma_1| |\Sigma_2|}} \right)$$

A representative GMM for the reference image can be obtained via the EM algorithm [4]. Therefore, the reference image is represented by the parameters $\Theta_k^{ref} = \{\mu_k^{ref}, \Sigma_k^{ref}\}$, $k = 1, \dots, K$ of the GMM components. After projecting the pixel groups of the reference image to obtain the corresponding groups in the registered image, it is easy to compute the parameters Θ_k^{reg} by taking the sample mean μ_k^{reg} and the sample covariance matrix Σ_k^{reg} :

$$\mu_k^{reg} = \frac{1}{|P_k|} \sum_{i=1}^{N^2} I_{reg}(T_S(x^i)) \delta(f(x^i) - k) \quad (3)$$

and

$$\Sigma_k^{reg} = \frac{1}{|P_k|} \sum_{i=1}^{N^2} (\Delta I_k^i) (\Delta I_k^i)^T \delta(f(x^i) - k), \quad (4)$$

where $\Delta I_k^i = I_{reg}(T_S(x^i)) - \mu_k^{reg}$. The role of $\delta(f(x^i) - k)$ in eq. (3) and (4) is to determine the support (the pixel coordinates) for the calculation of the mean and covariance. These parameters are computed *on the image to be registered* for the pixel coordinates belonging to the k^{th} class *on the reference image*. This also implies a Gaussian generative model for the components of I_{reg} . The total distance between the two images is computed using eq. (2), where the Bhattacharyya distance between the corresponding Gaussian components is considered as distance measure D .

However, in order to overcome the drawbacks of GMMs concerning outlying image data, we have employed in our registration method mixtures of Student's t -distributions as described in the next section.

3. Robust image registration with mixtures of Student's t -distributions

In what follows, we briefly present the properties of mixtures of t -distributions (SMMs), as well as ML estimation of their parameters using the EM algorithm. Then, we describe how SMMs can be employed as mixture models in the general registration approach presented in the previous section.

3.1. ML estimation of mixtures of Student's t -distributions

A d -dimensional random variable X follows a multivariate t -distribution with mean μ , positive definite, symmetric and real $d \times d$ covariance matrix Σ and has $\nu \in [0, \infty)$ degrees of freedom when, given the weight u , the variable X has the multivariate normal distribution with mean μ and covariance Σ/u :

$$X|\mu, \Sigma, \nu, u \sim N(\mu, \Sigma/u),$$

and the weight u follows a Gamma distribution parameterized by ν :

$$u \sim \text{Gamma}(\nu/2, \nu/2).$$

Integrating out the weights from the joint density leads to the density function of the marginal distribution:

$$p(x; \mu, \Sigma, \nu) = \frac{\Gamma(\frac{\nu+d}{2}) |\Sigma|^{-\frac{1}{2}}}{(\pi\nu)^{\frac{d}{2}} \Gamma(\frac{\nu}{2}) [1 + \nu^{-1} \delta(x, \mu; \Sigma)]^{\frac{\nu+d}{2}}} \quad (5)$$

where $\delta(x, \mu; \Sigma) = (x - \mu)^T \Sigma^{-1} (x - \mu)$ is the Mahalanobis squared distance and Γ is the Gamma function. It can be shown that for $\nu \rightarrow \infty$ the Student's t -distribution tends to a Gaussian distribution with covariance Σ . Also, if $\nu > 1$, μ is the mean of X and if $\nu > 2$, $\nu(\nu - 2)^{-1} \Sigma$ is the covariance matrix of X . Therefore, the family of t -distributions provides a heavy-tailed alternative to the normal family with mean μ and covariance matrix that is equal to a scalar multiple of Σ , if $\nu > 2$ (fig. 1).

A Student's t -distribution mixture model (SMM) may also be trained using the EM algorithm [23]. A K -component mixture of t -distributions is given by

$$\phi(x, \Psi) = \sum_{i=1}^K \pi_i p(x; \mu_i, \Sigma_i, \nu_i) \quad (6)$$

where $x = (x_1, \dots, x_N)^T$ denotes the observed-data vector and

$$\Psi = (\pi_1, \dots, \pi_K, \mu_1, \dots, \mu_K, \Sigma_1, \dots, \Sigma_K, \nu_1, \dots, \nu_K)^T. \quad (7)$$

are the parameters of the components of the mixture.

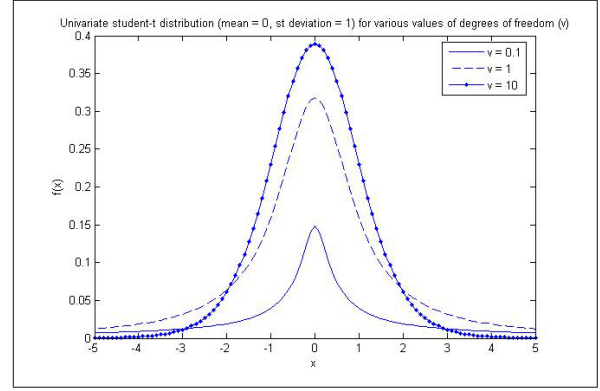


Figure 1. The Student's t -distribution for various degrees of freedom. As $\nu \rightarrow \infty$ the distribution tends to a Gaussian. For small values of ν the distribution has heavier tails than a Gaussian.

Consider now the complete data vector

$$x_c = (x_1, \dots, x_N, z_1, \dots, z_N, u_1, \dots, u_N)^T \quad (8)$$

where z_1, \dots, z_N are the component-label vectors and $z_{ij} = (z_j)_i$ is either one or zero, according to whether the observation x_j is generated or not by the i^{th} component. In the light of the definition of the t -distribution, it is convenient to view that the observed data augmented by the z_j , $j = 1, \dots, N$ are still incomplete because the component covariance matrices depend on the degrees of freedom. This is the reason that the complete-data vector also includes the additional missing data u_1, \dots, u_N . Thus, the E-step on the $(t + 1)^{\text{th}}$ iteration of the EM algorithm requires the calculation of the posterior probability that the datum x_j belongs to the i^{th} component of the mixture:

$$z_{ij}^{t+1} = \frac{\pi_i^t p(x_j; \mu_i^t, \Sigma_i^t, \nu_i^t)}{\sum_{m=1}^K p(x_j; \mu_m^t, \Sigma_m^t, \nu_m^t)} \quad (9)$$

as well as the expectation of the weights for each observation:

$$u_{ij}^{t+1} = \frac{\nu_i^t + d}{\nu_i^t + \delta(x_j, \mu_i^t; \Sigma_i^t)} \quad (10)$$

Maximizing the log-likelihood of the complete data provides the update equations of the respective mixture model parameters:

$$\pi_i^{t+1} = \frac{1}{N} \sum_{j=1}^N z_{ij}^t, \quad \mu_i^{t+1} = \frac{\sum_{j=1}^N z_{ij}^t u_{ij}^t x_j}{\sum_{j=1}^N z_{ij}^t u_{ij}^t}, \quad (11)$$

$$\Sigma_i^{t+1} = \frac{\sum_{j=1}^N z_{ij}^t u_{ij}^t (x_j - \mu_i^{t+1})(x_j - \mu_i^{t+1})^T}{\sum_{j=1}^N z_{ij}^{t+1}}. \quad (12)$$

The degrees of freedom for each component are computed as the solution to the equation:

$$\begin{aligned} \log\left(\frac{\nu_i^{t+1}}{2}\right) - \psi\left(\frac{\nu_i^{t+1}}{2}\right) + 1 - \log\left(\frac{\nu_i^t + d}{2}\right) + \\ + \frac{\sum_{j=1}^N z_{ij}^t (\log u_{ij}^t - u_{ij}^t)}{\sum_{j=1}^N z_{ij}^t} + \psi\left(\frac{\nu_i^t + d}{2}\right) = 0 \end{aligned} \quad (13)$$

where $\psi(x) = \frac{\partial(\ln\Gamma(x))}{\partial x}$ is the digamma function. A detailed derivation of the EM algorithm for Student's t -mixtures is presented in [23].

3.2. Implementation

The Student's t -distribution is a heavy tailed approximation to the Gaussian. It is therefore, natural to consider the mean and covariance of the SMM components to approximate the parameters of a GMM on the same data as it was described in the previous section. If the images follow a Gaussian model, the degrees of freedom ν_i are relatively large and the SMM tends to be a GMM with the same parameters. If the images contain outliers, parameters ν_i are weak and the mean and covariance of the data are appropriately weighted in order not to take into account the outliers. Thus, the parameters of the SMM, computed on the reference image I_{ref} , are used as component parameters Θ_k^{ref} in a straightforward way as they generalize the Gaussian case by correctly addressing the outliers problem. After projection of the pixel groups of the reference image to their corresponding groups in the registered image, the parameters Θ_k^{reg} are computed using the sample mean (3) and the sample covariance matrix (4).

The Iterated Conditional Modes (ICM) [2] algorithm was implemented for the minimization of the energy function as (2) is highly non-linear. ICM is a deterministic Gauss-Seidel like algorithm, that only accepts configurations decreasing the cost function and has fast convergence properties. If good initialization is provided, Powell's method also converges fast to the correct solution without having to compute derivatives of the objective function (2) with respect to the transformation parameters.

A large number of interpolations are involved in the registration process. The accuracy of the rotation and translation parameter estimates is directly related to the accuracy

of the underlying interpolation model. Simple approaches such as the nearest neighbor interpolation are commonly used because they are fast and simple to implement, though they produce images with noticeable artifacts. More satisfactory results can be obtained by small-kernel cubic convolution techniques. In our experiments, we have applied a bilinear interpolation scheme, thus preserving the quality of the image to be registered.

Finally, let us notice that the energy in (2) may be applied to both single and multimodal image registration. In the latter case, the difference in the mean values of the distributions in (2) should be ignored, as we do not search to match the corresponding Student's t -distributions in position but only in shape as the correspondence in position is established by the projection step. This also stands for the single modal case if the intensities of the image pair have significantly different contrasts.

4. Experimental results

In order to evaluate the proposed method, we have performed a number of experiments in some relatively difficult registration problems. Registration errors were computed in terms of pixels and not in terms of transformation parameters. Registration accuracies in terms of rotation angles and translation vectors are not easily evaluated due to parameter coupling. Therefore, the registration errors are defined as deviations of the corners of the registered image with respect to the ground truth position. Let us notice that these registration errors are less forgiving at the corners of the image (where their values are larger) with regard to the center of the image frame.

At first, we have applied our method to the registration of a piecewise constant image with three distinct regions to its noisy and rigidly transformed counterpart. Knowing the number of mixture components allows better evaluation of the method with respect to noise. The image in fig. 2(a) was degraded by uniformly distributed noise in order to achieve various SNR values between 8.5 dB and 3.2 dB by appropriately varying the standard deviation of the noise. An example is shown in fig. 2(b). The degraded images underwent several rigid transformations by rotation angles varying between $[-45, 45]$ degrees and translation parameters between $[-10, 10]$ pixels. To investigate the robustness the proposed method to outliers we have applied the algorithm with $K = 3$ components considering both GMMs and SMMs. Figure 3 illustrates the average registration errors for the different SNR values. For each SNR, 10 different transformations were applied to the image and the average value of the registration error is presented. For comparison purposes, the performance of the MI method is also shown. As it can be observed, both the GMM and the SMM-based registration methods outperform the MI which fails when the SNR is low. Moreover, the heavier

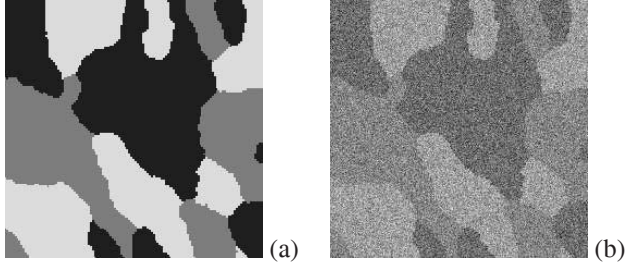


Figure 2. (a) A three-class piecewise constant image with intensity values 30, 125 and 220. (b) The image degraded by zero mean uniform noise in order to achieve a SNR of 3.2 dB.

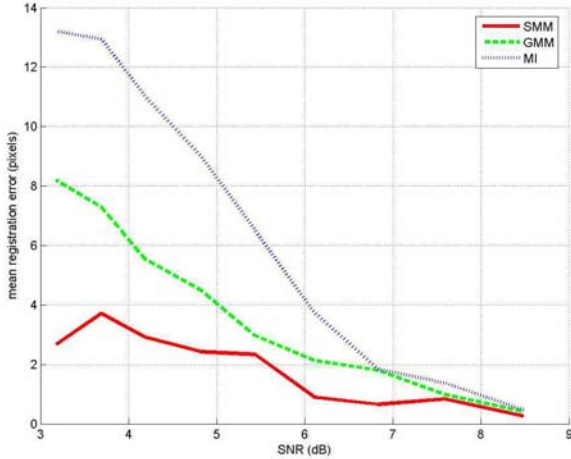


Figure 3. Mean registration error versus signal to noise ratio (SNR) for the 3-class registration experiment of figure 2.

tailed SMM demonstrates better performance for considerable amounts of noise. When the SNR is higher than 8 dB, all methods provide correct registrations.

The proposed registration method was also tested on multimodal image pairs such as the MRI/SPECT case in fig. 4 and the cell images in fig. 5. The complimentary but not redundant information carried by the multimodal images increases the difficulty of the registration process. In both experiments we have applied 25 rigid transformations to one of the images with rotation angles varying between $[-45, 45]$ degrees and translation parameters between $[-20, 20]$ pixels. The experiments were realized with the number of components being $K = 2, \dots, 10$ and $K = 16$. Table 1 summarizes the statistics on the registration errors for the number of components that provided the better performances. These values are $K = 5$ in the case of MRI/SPECT and $K = 6$ for the cell images. As it can be observed, the SMM method achieves sub-pixel accuracy in all cases.

A last experiment demonstrating the performance of the

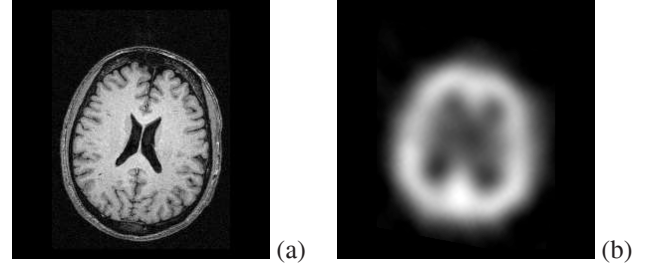


Figure 4. (a) A slice of a brain MR image and (b) its SPECT counterpart used in our experiments. Notice the important diffusion present in the SPECT image.

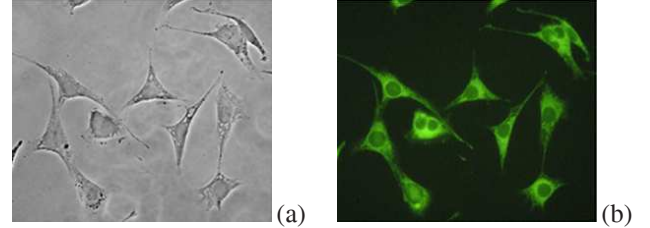


Figure 5. A pair of NIH 3T3 electron microscope images (400x magnification) of rat cells under (a) normal and (b) fluorescent light.

SMM Registration errors - Multimodal images		
	MRI/SPECT	Cell images
Mean	0.50	0.27
St. dev.	0.47	0.11
Median	0.55	0.32
Min	0.07	0.08
Max	1.92	1.06

Table 1. Statistics on the registration errors for the images in fig. 4 and 5. The errors are expressed in pixels. The number of SMM components is $K = 5$ for the brain and $K = 6$ for the cell images.

proposed SMM method to deal with outliers is the registration of a remotely sensed image pair. The meteorological images of Europe in fig. 6 were acquired at different dates. The image in fig. 6(b) underwent 25 rigid transformation with values of rotation angle uniformly sampled in the interval $[-45, 45]$ degrees and translations between $[-10, 10]$ pixels. The experiments were realized with the number of components being $K = 2, \dots, 10$ and $K = 16$. For the MI case, where K is the number of histogram bins, the values of $K = \{128, 256\}$ were also used in order to have the best possible performance. The large amount of clouds at different locations in the image pair introduce difficulties in the registration procedure. It is worth commenting that the MI method failed to register the images and systematically provided registration errors of the order of 7 to 10 pixels. This is true even for a large numbers of histogram bins. The SMM method produced very small registration errors which are summarized in table 2.

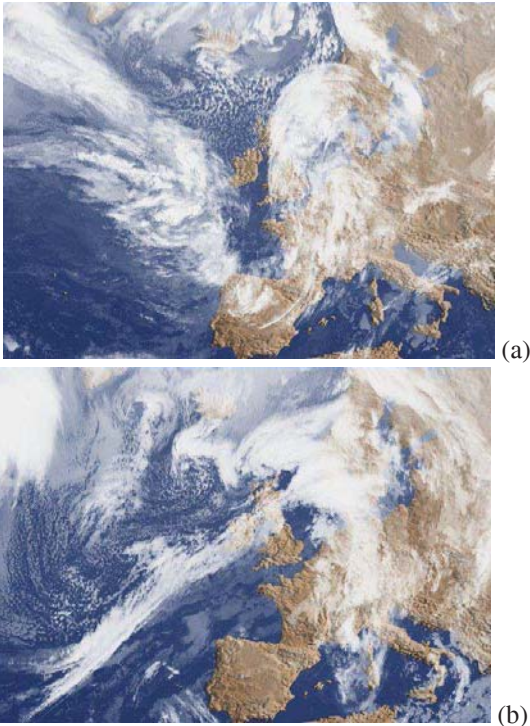


Figure 6. (a) Image of Europe on 8 January 2007 at 01h00, provided by MeteoSat. (b) Image of Europe on 9 January 2007 at 01h00, provided by MeteoSat (by courtesy of Meteo-France). Notice the large amount of outliers (cloudy regions in different locations in the image pair) introducing important difficulties in the registration process.

Registration errors - Satellite images		
	MI	SMM
Mean	7.12	0.88
St. dev.	2.66	0.63
Median	6.40	0.67
Min	3.61	0.21
Max	11.37	1.69

Table 2. Statistics on the registration errors for the images in fig. 6. The errors are expressed in pixels. Notice that the MI failed to correctly register the images.

5. Conclusion

We have presented a method for the registration of single and multimodal images. The method relies on the minimization of distances between probability density functions defined by partitioning the two images. The first image is partitioned by a SMM through the EM algorithm. This partition is then implied onto the second image. We have shown the effectiveness and accuracy of the proposed method especially with images presenting dissimilarities, such as the remotely sensed image pair, where the mutual information method fails to correctly register the two images. Vector valued (RGB, textured or multispectral)

images are expected to benefit from this registration technique where the employment of high-dimensional joint histograms makes the use of standard methods prohibitive.

Let us also notice that Student's t -mixtures overcome the binning problem of histogram-based methods and provide a continuous model of the image density. When successfully trained, they produce a sensible approximation of the pdf of the image intensity, by placing density components in a sensible *data-driven* way (i.e on intensity regions exhibiting high density). Although there is still the problem of specifying the number of components in finite mixture modeling, our experimental results indicated that our SMM-based method is robust from this point of view, provided that the number of components is neither very big (overfitting) nor very small (underfitting).

Important open questions for mixture-based registration are how the number of model components can be selected automatically [5] and which features, apart from image intensity, should be used [6]. Moreover, the generalization of the proposed method to the registration of scattered data [15, 21] is a perspective of our study. The difficulty in that case consists in establishing the correspondences between the components of the mixture between the two point sets [15].

Acknowledgements

The authors wish to thank Prof. Th. Tzavaras, Laboratory of General Biology, School of Medicine, University of Ioannina, for providing the cell images and Dr. J. P. Armspach, Institut de Physique Biologique, Université Louis Pasteur, Strasbourg, France, for providing the MRI/SPECT images.

References

- [1] I. Bankman, editor. *Handbook of medical image processing and analysis*. Academic Press, 2000. 1
- [2] J. Besag. On the statistical analysis of dirty pictures. *Journal of the Royal Statistical Society*, 48(3):259–302, 1986. 5
- [3] C. Bishop and M. Svensen. Robust Bayesian mixture modelling. In *Proceedings of the 12th European Symposium on Artificial Neural Networks (ESANN'04)*, Bruges, Belgium, 2004. 2
- [4] C. M. Bishop. *Pattern Recognition and Machine Learning*. Springer, 2006. 1, 3
- [5] S. Chen, H. Wang, and B. Luo. Greedy EM algorithm for robust t -mixture modeling. In *Proceedings of the 3rd IEEE International Conference on Imaging and Graphics (ICIG'04)*, Hong-Kong, China, 2004. 7
- [6] C. Constantinopoulos, M. K. Titsias, and A. Likas. Bayesian feature and model selection for Gaussian

- mixture models. *IEEE Transactions on Pattern Analysis and Machine Intelligence*, 28(6):1013–1018, 2006. 7
- [7] K. Fukunaga. *Introduction to statistical pattern recognition*. Academic Press, 1990. 3
- [8] A. Guimond, A. Roche, N. Ayache, and J. Meunier. Three-dimensional multimodal brain warping using the demons algorithm and adaptive intensity corrections. *IEEE Transactions on Medical Imaging*, 20(1):58–69, 2001. 2
- [9] J. V. Hajnal, D. L. G. Hill, and D. J. Hawkes. *Medical image registration*. CRC Press, 2001. 1
- [10] F. Heitz, H. Maître, and C. de Couessin. Event detection in multisource imaging: application to fine arts painting analysis. *IEEE Transactions on Acoustic, Speech and Signal Processing*, 38(4):695–704, 1990. 1
- [11] P. Hellier. Consistent intensity correction of MR images. In *Proceedings of the 2003 IEEE International Conference on Image Processing (ICIP'03)*, volume 1, pages 1109–1112, Barcelona, Spain, 2003. 2
- [12] M. Herbin, A. Venot, J. Y. Devaux, E. Walter, F. Lebruchec, L. Dubertet, and J. C. Roucayrol. Automated registration of dissimilar images: application to medical imagery. *Computer Vision, Graphics and Image Processing*, 47:77–88, 1989. 2
- [13] G. Hermosillo and O. Faugeras. Dense image matching with global and local statistical criteria. In *Proceedings of the 2001 IEEE Conference on Computer Vision and Pattern Recognition (CVPR'01)*, volume 1, pages 73–78, Los Alamitos, USA, 2001. 1
- [14] J. R. Jensen. *Introductory digital image processing: a remote sensing perspective*. Prentice Hall, 3rd edition, 2004. 1
- [15] B. Jian and B. C. Vemuri. A robust algorithm for point set registration using mixture of Gaussians. In *Proceedings of the 10th International Conference on Computer Vision (ICCV'05)*, pages 1246–1251, Beijing, China, 2005. 2, 7
- [16] M. Leventon and E. Grimson. Multi-modal volume registration using joint intensity distributions. In *Proceedings of the Medical Image Computing and Computer Assisted Intervention Conference (MICCAI'98)*, pages 1057–1066, Cambridge, Massachusetts, USA, October 1998. 1
- [17] F. Maes, A. Collignon, D. Vandermeulen, G. Marchal, and P. Suetens. Multimodality image registration by maximization of mutual information. *IEEE Transactions on Medical Imaging*, 16(2):187–198, 1997. 1
- [18] J. B. A. Maintz and M. A. Viergever. A survey of medical image registration techniques. *Medical Image Analysis*, 2(1):1–36, 1998. 1
- [19] D. Mattes, D. R. Haynor, H. Vesselle, T. K. Lewellen, and W. Eubank. Nonrigid multimodality image registration. In K. Hanson, editor, *Proceedings of the 2001 SPIE Medical Imaging Conference*, volume 4322, pages 1609–1620, San Diego, USA, 2003. 1
- [20] G. McLachlan. *Finite mixture models*. Wiley-Interscience, 2000. 1, 2
- [21] A. Myronenko, X. Song, and M. Á. Carreira-Perpiñán. Non-rigid point set registration: Coherent Point Drift. In B. Schölkopf, J. Platt, and T. Hoffman, editors, *Proceedings of the 20th Conference on Advances in Neural Information Processing Systems (NIPS'06)*. MIT Press, Vancouver, Canada, 2006. 7
- [22] C. Nikou, F. Heitz, and J. P. Armspach. Robust voxel similarity metrics for the registration of dissimilar single and multimodal images. *Pattern Recognition*, 32:1351–1368, 1999. 1, 2
- [23] D. Peel and G. J. McLachlan. Robust mixture modeling using the *t*-distribution. *Statistics and Computing*, 10:339–348, 2000. 2, 4, 5
- [24] J. Pluim, J. B. A. Maintz, and M. Viergever. Mutual information based registration of medical images: a survey. *IEEE Transactions on Medical Imaging*, 22(8):986–1004, 2004. 1
- [25] A. Rajwade, A. Banerjee, and A. Rangarajan. A new method of probability density estimation with application to mutual information based image registration. In *Proceedings of the 2006 IEEE Conference on Computer Vision and Pattern Recognition (CVPR'06)*, New York, USA, 2006. 1
- [26] A. Roche, X. Pennec, G. Malandain, and N. Ayache. Rigid registration of 3-D ultrasound with MR images: a new approach combining intensity and gradient information. *IEEE Transactions on Medical Imaging*, 20(10):1038–1049, 2001. 2
- [27] P. Thévenaz and M. Unser. Optimization of mutual information for multiresolution image registration. *IEEE Transactions on Image Processing*, 9(12):2083–2099, 2000. 1
- [28] P. Viola and W. Wells III. Alignment by maximization of mutual information. *International Journal of Computer Vision*, 24(2):137–154, 1997. 1
- [29] B. Zitova and J. Flusser. Image registration methods: a survey. *Image and Vision Computing*, 21(11):1–36, 2003. 1